Perfectly Matched Layers in the Discretized Space: An Analysis and Optimization †

W. C. Chew and J. M. Jin
Center for Computational Electromagnetics
Electromagnetics Laboratory
Department of Electrical and Computer Engineering
University of Illinois
Urbana, IL 61801

Abstract

The perfectly matched layer (PML) has recently been introduced by Berenger as a material absorbing boundary condition (ABC) for electromagnetic waves. Recently, it has been pointed out that this absorbing boundary condition is the same as coordinate stretching in the complex space. In this paper, the corresponding coordinate stretching is analyzed in the discretized space of Maxwell's equations as described by the Yee algorithm. The corresponding dispersion relationship is derived for a PML medium and then the problem of reflection from a single interface is solved. A perfectly matched interface is shown not to exist in the discretized space, even though it exists in the continuum space. Numerical simulations both using finite difference method and finite element method confirm that such discretization error exists. A numerical scheme using the finite element method is then developed to optimize the PML with respect to its parameters. Examples are given to demonstrate the performance of the optimized PML and its application to the finite element solution of scattering problems.

1. Introduction

The perfectly matched layer (PML) as a material absorbing boundary condition (MABC) has been recently introduced for electromagnetic waves by Berenger (1994). This material absorbing boundary condition holds great promise for truncating the mesh in the numerical solution of the partial differential equations of wave scattering.

Various workers have sought a different interpretation of this material absorbing boundary conditions (Chew and Weedon, 1994; Katz et al., 1994; Navarro et al., 1994; Mittra and Pekel, 1995; Sacks et al., 1995; Chew et al., 1995; Gribbons et al., 1995). Work on it has also been extended to three dimensions. Recently, Chew and Weedon (1994) have interpreted the perfectly matched layers as coordinate stretching in frequency domain. Since the stretching variables are complex, they necessitate the splitting of Maxwell's equations in the time domain. The PML is shown to be of very wide bandwidth, and is capable of absorbing static electromagnetic fields as well (Chew et al., 1995).

A perfectly matched interface is an interface between two half spaces, one of which is lossy, but the interface does not reflect a plane wave for all frequencies and all angles of incidence. The loss of the wave in the lossy half space is in the

† This work was supported by Office of Naval Research under grants N00014-95-1-0872 and N00014-95-1-0848, and the National Science Foundation under grants NSF ECS 93-02145 and ECS 94-57735. WCC thanks Eric Michielssen for identifying some inconsistencies in his program. This paper was presented at the 1995 URSI Meeting, Newport Beach, and published in *Electromagnetics,* vol. 16, no. 4, pp.325-340, 1996.

direction normal to the interface. As such, the PML medium has been touted as the best absorbing boundary condition for numerical solution of partial differential equations.

In this paper, the PML medium will be analyzed in the discretized space as described by the Yee algorithm—the most popular finite difference time domain algorithm for solving Maxwell's equations in the discretized space (Yee, 1966). The dispersion relationship will be derived for a plane wave in a discretized PML medium. Then the plane wave reflection of the single interface problem between two PML media will be solved. It will be shown that a perfectly matched interface does not exist between two PML media in the discretized space. This will be corroborated by numerical simulation using finite difference method as well as finite element method (Chew, 1990; Jin, 1993). After that, a numerical scheme will be developed to optimize the PML with respect to its parameters. Numerical examples will be given to demonstrate the performance of the optimized PML and its application to the finite element solution of scattering problems.

2. Formulation

The split Maxwell's equations in the time domain are (Chew and Weedon, 1994)

$$a_x \mu \partial_t \mathbf{H}_{sx} + \Omega_x \mu \mathbf{H}_{sx} = -\partial_x \hat{x} \times \mathbf{E}, \tag{1}$$

$$a_x \epsilon \partial_t \mathbf{E}_{sx} + \Omega_x \epsilon \mathbf{E}_{sx} = \partial_x \hat{x} \times \mathbf{H}. \tag{2}$$

Another four equations could be derived by replacing x above by y or z. Using the notation in (Chew, 1994), the above can be rewritten as

$$(\hat{a}_x \hat{\mu})_{\mathbf{m}+\frac{1}{2}} \tilde{\partial}_t \hat{\mathbf{H}}^{l-\frac{1}{2}}_{sx,\mathbf{m}+\frac{1}{2}} + \left(\hat{\Omega}_x \hat{\mu}\right)_{\mathbf{m}+\frac{1}{2}} \hat{\mathbf{H}}^{l+\frac{1}{2}}_{sx,\mathbf{m}+\frac{1}{2}} = -\tilde{\partial}_x \hat{x} \times \tilde{\mathbf{E}}^l_{\mathbf{m}}, \tag{3}$$

$$(\tilde{a}_x \tilde{\epsilon})_{\mathbf{m}} \hat{\partial}_t \tilde{\mathbf{E}}^l_{sx,\mathbf{m}} + \left(\tilde{\Omega}_x \tilde{\epsilon}\right)_{\mathbf{m}} \tilde{\mathbf{E}}^l_{sx,\mathbf{m}} = \hat{\partial}_x \hat{x} \times \hat{\mathbf{H}}^{l-\frac{1}{2}}_{\mathbf{m}+\frac{1}{2}}. \tag{4}$$

In the above, $\mathbf{m} + \frac{1}{2} = (m + \frac{1}{2}; n + \frac{1}{2}; p + \frac{1}{2})$, and $\mathbf{m} = (m, n, p)$ denote the locations of the Yee's finite difference time domain (FDTD) grid points (Yee, 1966; Taflove, 1988). $\tilde{\partial}_t$ and $\tilde{\partial}_x$ are forward difference approximation of the ∂_t and ∂_x operators, and $\hat{\partial}_t$ and $\hat{\partial}_x$ are backward difference approximation of the same operators. $\hat{\mathbf{H}}$ denotes a back vector while $\tilde{\mathbf{E}}$ denotes a fore vector. Also, when a fore vector is associated with the node $\mathbf{m}$, the respective field components are associated with the respective branches forward to the node. For instance, the x component of $\tilde{\mathbf{E}}_{\mathbf{m}}$ is associated with the location $(m + \frac{1}{2}, n, p)$. A similar definition applies for a back vector. For instance, the x component of $\hat{\mathbf{H}}_{\mathbf{m}+\frac{1}{2}}$ is associated with the locations $(m, n + \frac{1}{2}, p + \frac{1}{2})$. The tilde and hat over a_x, ϵ, μ, and Ω_x indicate that they are to be evaluated at the location of the fore vector and back vector, respectively, they are associated with.

The above is similar to the use of Yee algorithm for implementing (1) and (2) by the finite difference method (Chew, 1994).

The equations above correspond to the lossy wave equation. However, when the term associated with $\tilde{\partial}_t$ or $\hat{\partial}_t$ is zero, the equations become diffusive (Chew, 1995). The time steps for the terms associated with $\Omega_x \mu$ and $\Omega_x \epsilon$ are chosen to ensure stability when the equations become purely diffusive. A sufficient condition for stability is to ensure that the time step satisfies the CFL condition (Chew, 1995).

Next, a time harmonic plane wave is assumed such that

$$\tilde{\mathbf{E}}^l_{\mathbf{m}} = \tilde{\mathbf{E}}_{\mathbf{m}} e^{-i\omega l \Delta_t}, \quad \hat{\mathbf{H}}^{l-\frac{1}{2}}_{\mathbf{m}+\frac{1}{2}} = \hat{\mathbf{H}}_{\mathbf{m}+\frac{1}{2}} e^{-i\omega l \Delta_t}, \tag{5}$$

where Δ_t is the time-stepping size. Then in (3) and (4), the difference operators become (Chew, 1994)

$$\tilde{\partial}_t \Rightarrow -i\tilde{\Omega}_t, \quad \hat{\partial}_t \Rightarrow -i\hat{\Omega}_t \tag{6}$$

where

$$\tilde{\Omega}_t = \omega \mathrm{sinc}(\delta_t) e^{-i\delta_t}, \quad \hat{\Omega}_t = \omega \mathrm{sinc}(\delta_t) e^{i\delta_t}, \tag{7}$$

and $\delta_t = \omega\Delta_t/2$. Consequently, for a time harmonic field, (3) and (4) become

$$\left(-i\tilde{\Omega}_t a_x + \hat{\Omega}_x e^{-2i\delta_t}\right)_{\mathbf{m}+\frac{1}{2}} \mu_{\mathbf{m}+\frac{1}{2}} \hat{\mathbf{H}}_{sx,\mathbf{m}+\frac{1}{2}} = -\tilde{\partial}_x \hat{x} \times \tilde{\mathbf{E}}_{\mathbf{m}}, \tag{8a}$$

$$\left(-i\hat{\Omega}_t a_x + \tilde{\Omega}_x\right)_{\mathbf{m}} \epsilon_{\mathbf{m}} \tilde{\mathbf{E}}_{sx,\mathbf{m}} = \hat{\partial}_x \hat{x} \times \hat{\mathbf{H}}_{\mathbf{m}+\frac{1}{2}}. \tag{8b}$$

The above could be written as

$$i\tilde{\Omega}_t (\hat{S}_x \hat{\mu})_{\mathbf{m}+\frac{1}{2}} \hat{\mathbf{H}}_{sx,\mathbf{m}+\frac{1}{2}} = \tilde{\partial}_x \hat{x} \times \tilde{\mathbf{E}}_{\mathbf{m}}, \tag{9a}$$

$$-i\hat{\Omega}_t (\tilde{S}_x \tilde{\epsilon})_{\mathbf{m}} \tilde{\mathbf{E}}_{sx,\mathbf{m}} = \hat{\partial}_x \hat{x} \times \hat{\mathbf{H}}_{\mathbf{m}+\frac{1}{2}}, \tag{9b}$$

where $S_x = a_x + i\Omega_x/\hat{\Omega}_t$. The ratio $\Omega_x/(\hat{\Omega}_t a_x)$ is like the loss tangent of the PML medium. In the above, the hat over S_x and μ implies that they are to be evaluated at the same locations as the components of $\hat{\mathbf{H}}$, and similarly, for tilde over the same scalar quantities, they are to be evaluated at the same locations as the components of $\tilde{\mathbf{E}}$.

Repeating the above for y and z, and combining the resultant equations, one obtains

$$i\tilde{\Omega}_t \hat{\mu}_{\mathbf{m}+\frac{1}{2}} \hat{\mathbf{H}}_{\mathbf{m}+\frac{1}{2}} = \tilde{\nabla}_e \times \tilde{\mathbf{E}}_{\mathbf{m}}, \tag{10a}$$

$$-i\hat{\Omega}_t \tilde{\epsilon}_{\mathbf{m}} \tilde{\mathbf{E}}_{\mathbf{m}} = \hat{\nabla}_e \times \hat{\mathbf{H}}_{\mathbf{m}+\frac{1}{2}}, \tag{10b}$$

where

$$\tilde{\nabla}_e = \hat{x}\frac{1}{\hat{S}_x}\tilde{\partial}_x + \hat{y}\frac{1}{\hat{S}_y}\tilde{\partial}_y + \hat{z}\frac{1}{\hat{S}_z}\tilde{\partial}_z, \quad \hat{\nabla}_e = \hat{x}\frac{1}{\tilde{S}_x}\hat{\partial}_x + \hat{y}\frac{1}{\tilde{S}_y}\tilde{\partial}_y + \hat{z}\frac{1}{\tilde{S}_z}\tilde{\partial}_z. \tag{11}$$

Equations (10) are valid for inhomogeneous media as well. In this case, one needs to be cautioned on the interpretation of S_ξ, $\xi = x, y, z$.

For a homogeneous medium, a plane wave solution may be assumed such that

$$\tilde{\mathbf{E}}_{\mathbf{m}} = \tilde{\mathbf{E}}_0 e^{i\mathbf{k}\cdot\mathbf{r}}, \quad \hat{\mathbf{H}}_{\mathbf{m}+\frac{1}{2}} = \hat{\mathbf{H}}_0 e^{i\mathbf{k}\cdot\mathbf{r}}, \tag{12}$$

where, $\mathbf{k} = \hat{x}k_x + \hat{y}k_y + \hat{z}k_z$, and $\mathbf{r} = \hat{x}x + \hat{y}y + \hat{z}z, x = m\Delta_x, y = n\Delta_y, z = p\Delta_z$. Using this in (10), one arrives at

$$\tilde{\Omega}_t \mu \hat{\mathbf{H}}_0 = \tilde{\mathbf{K}}_e \times \tilde{\mathbf{E}}_0, \quad -\hat{\Omega}_t \epsilon \tilde{\mathbf{E}}_0 = \hat{\mathbf{K}}_e \times \hat{\mathbf{H}}_0. \tag{13}$$

where

$$\tilde{\mathbf{K}}_e = \hat{x}\frac{\tilde{K}_x}{S_x} + \hat{y}\frac{\tilde{K}_y}{S_y} + \hat{z}\frac{\tilde{K}_z}{S_z}, \tag{14a}$$

$$\hat{\mathbf{K}}_e = \hat{x}\frac{\hat{K}_x}{S_x} + \hat{y}\frac{\hat{K}_y}{S_y} + \hat{z}\frac{\hat{K}_z}{S_z}, \tag{14b}$$

and

$$\tilde{K}_\xi = k_\xi \text{sinc}(\delta_\xi) e^{i\delta_\xi}, \quad \hat{K}_\xi = k_\xi \text{sinc}(\delta_\xi) e^{-i\delta_\xi}, \quad \xi = x, y, z \tag{15}$$

where $\delta_\xi = k_\xi \Delta_\xi / 2$, and Δ_ξ is the space discretization size. Combining the equations in (13), one has

$$-\Omega_t^2 \mu\epsilon \hat{\mathbf{H}}_0 = \tilde{\mathbf{K}}_e \times \hat{\mathbf{K}}_e \times \hat{\mathbf{H}}_0 = \hat{\mathbf{K}}_e (\tilde{\mathbf{K}}_e \cdot \hat{\mathbf{H}}_0) - \tilde{\mathbf{K}}_e \cdot \hat{\mathbf{K}}_e \hat{\mathbf{H}}_0 \tag{16}$$

where, $\Omega_t = \omega \text{sinc}(\delta_t)$. Since from (13), $\tilde{\mathbf{K}}_e \cdot \hat{\mathbf{H}}_0 = 0$, and hence,

$$\Omega_t^2 \mu\epsilon = \tilde{\mathbf{K}}_e \cdot \hat{\mathbf{K}}_e. \tag{17}$$

More specifically, the above reduces to

$$K^2 = \frac{1}{S_x^2} K_x^2 + \frac{1}{S_y^2} K_y^2 + \frac{1}{S_z^2} K_z^2, \tag{18}$$

where $K^2 = \Omega_t^2 \mu\epsilon$, $K_\xi = k_\xi \text{sinc}(\delta_\xi)$, $\xi = x, y, z$.

Equation (18) can be satisfied by

$$K_x = K S_x \sin\theta \cos\phi, \quad K_y = K S_y \sin\theta \sin\phi, \quad K_z = K S_z \cos\theta. \tag{19}$$

Notice that S_x, S_y, and S_z are complex so that K_x, K_y, and K_z are complex even if the rest of the numbers are real. In other words, the loss of the medium can be controlled independently in the x, y, and z directions by various choices of the complex stretching variables S_ξ. One should note the parallel of this analysis compared to the continuum space case (Chew and Weedon, 1994).

The above represents the theory of Yee algorithm in a homogeneous PML medium. To establish the stability of the method, one can solve for Ω_t from (18) given the value of K_x, K_y, and K_z, and hence the value of ω. If the roots are such that ω is in the upper half complex plane, then the FDTD scheme is unstable.

3. Single Interface Reflection Problem

The previous section discussed the PML theory for homogeneous media in a discretized space. Next, we like to formulate the theory in the discretized space for a single-interface problem consisting of a planar interface separating two homogeneous half spaces. To this end, a TE incident wave is assumed in region 1 and the waves in regions 1 and 2 are written as (Chew and Weedon, 1994)

$$\tilde{\mathbf{E}}_1 = \tilde{\mathbf{E}}_0 e^{i\mathbf{k}_i \cdot \mathbf{r}} + R^{TE} \tilde{\mathbf{E}}_{0r} e^{i\mathbf{k}_r \cdot \mathbf{r}}, \tag{20a}$$

$$\tilde{\mathbf{E}}_2 = T^{TE} \tilde{\mathbf{E}}_{0t} e^{i\mathbf{k}_t \cdot \mathbf{r}}, \tag{20b}$$

where $\mathbf{k}_i = \hat{x}k_{ix} + \hat{y}k_{iy} - \hat{z}k_{iz}$, $\mathbf{k}_r = \hat{x}k_{rx} + \hat{y}k_{ry} + \hat{z}k_{rz}$, R^{TE} and T^{TE} are reflection and transmission coefficients, respectively. Phase matching requires that $k_{ix} = k_{rx} = k_{tx}$, $k_{iy} = k_{ry} = k_{ty}$. Therefore, $k_{iz} = k_{rz} = k_{tz}$. Without loss of generality, we can let $\tilde{\mathbf{E}}_{0r} = \tilde{\mathbf{E}}_{0t} = \tilde{\mathbf{E}}_0$. Requiring that the tangential $\mathbf{E}$ field be continuous across an interface at $z = 0$, implies that

$$1 + R^{TE} = T^{TE}. \tag{21}$$

Using Equation (10), we have

$$\hat{\mathbf{H}}_1 = \frac{\tilde{\mathbf{K}}_{ie} \times \tilde{\mathbf{E}}_0}{\tilde{\Omega}_t \mu_1} e^{i\mathbf{k}_i \cdot \mathbf{r}} + R^{TE} \frac{\tilde{\mathbf{K}}_{re} \times \tilde{\mathbf{E}}_0}{\tilde{\Omega}_t \mu_1} e^{i\mathbf{k}_r \cdot \mathbf{r}}, \tag{22a}$$

$$\hat{\mathbf{H}}_2 = T^{TE} \frac{\tilde{\mathbf{K}}_{te} \times \tilde{\mathbf{E}}_0}{\tilde{\Omega}_t \mu_2} e^{i\mathbf{k}_t \cdot \mathbf{r}}. \tag{22b}$$

In the above,

$$\tilde{\mathbf{K}}_{ie} = \frac{\hat{x}}{S_{1x}} K_{1x} e^{i\delta_{1x}} + \frac{\hat{y}}{S_{1y}} K_{1y} e^{i\delta_{1y}} - \frac{\hat{z}}{S_{1z}} K_{1z} e^{-i\delta_{1z}}, \tag{23a}$$

$$\tilde{\mathbf{K}}_{re} = \frac{\hat{x}}{S_{1x}} K_{1x} e^{i\delta_{1x}} + \frac{\hat{y}}{S_{1y}} K_{1y} e^{i\delta_{1y}} + \frac{\hat{z}}{S_{1z}} K_{1z} e^{i\delta_{1z}}, \tag{23b}$$

$$\tilde{\mathbf{K}}_{te} = \frac{\hat{x}}{S_{2x}} K_{2x} e^{i\delta_{2x}} + \frac{\hat{y}}{S_{2y}} K_{2y} e^{i\delta_{2y}} - \frac{\hat{z}}{S_{2z}} K_{2z} e^{-i\delta_{2z}}, \tag{23c}$$

where $K_{i\xi} = k_{i\xi}\,\mathrm{sinc}(\delta_{i\xi})$, $\delta_{i\xi} = \frac{k_{i\xi}\Delta_\xi}{2}$, $i = 1, 2$, $\xi = x, y, z$. By phase matching, $K_{1x} = K_{2x}$, $K_{1y} = K_{2y}$, $\delta_{1x} = \delta_{2x}$, and $\delta_{1y} = \delta_{2y}$. From Equation (10), it can be shown

$$\hat{\partial}_z \hat{z} \times \hat{\mathbf{H}}_{\mathbf{m}+\frac{1}{2}} = \left(\frac{K_z^2}{i\tilde{\Omega}_t \mu S_z} \tilde{\mathbf{E}}_s \right)_{\mathbf{m}} \tag{24}$$

where $\tilde{\mathbf{E}}_s$ indicates components transverse to $\hat{z}$. The above implies that

$$\hat{z} \times (\hat{\mathbf{H}}_{p=\frac{1}{2}} - \hat{\mathbf{H}}_{p=-\frac{1}{2}}) = \left(\frac{K_z^2 \Delta_z}{i\tilde{\Omega}_t \mu S_z} \tilde{\mathbf{E}}_s \right)_{p=0} \tag{25}$$

where p is the discrete variable in the z direction, and $p = 0$ is the same as $z = 0$. The above is the boundary condition for the magnetic field for a material discontinuity at $z = 0$.

Extracting the tangential components of (22a) and (22b), and inserting into (25), we have

$$-\frac{1}{\mu_1 S_{1z}} \left(K_{1z} e^{-i\delta_{1z}} - R^{TE} K_{1z} e^{i\delta_{1z}} \right) + \frac{K_{2z}}{\mu_2 S_{2z}} T^{TE} = \left(\frac{iK_z^2 \Delta_z}{\mu S_z} \right)_{p=0} T^{TE}. \tag{26}$$

The above could be rearranged to yield

$$-\frac{K_{1z}}{\mu_1 S_{1z}} e^{-i\delta_{1z}} + R^{TE} \frac{K_{1z}}{\mu_1 S_{1z}} e^{i\delta_{1z}} = -T^{TE} \left[\frac{K_{2z} e^{i\delta_{2z}}}{\mu_2 S_{2z}} - i \left(\frac{K_z^2 \Delta_z}{\mu S_z} \right)_{p=0} \right]. \tag{27}$$

Solving (21) and (27) for R^{TE} and T^{TE} yields

$$R^{TE} = \frac{K_{1z} e^{-i\delta_{1z}}/(\mu_1 S_{1z}) - A}{K_{1z} e^{i\delta_{1z}}/(\mu_1 S_{1z}) + A}, \tag{28}$$

$$T^{TE} = \frac{K_{1z}/(\mu_1 S_{1z}) \left[e^{i\delta_{1z}} + e^{-i\delta_{1z}} \right]}{K_{1z} e^{i\delta_{1z}}/(\mu_1 S_{1z}) + A}, \tag{29}$$

where $K_{1z} = k_{1z}\mathrm{sinc}(\delta_{1z})$, and

$$A = \frac{K_{2z}e^{i\delta_{2z}}}{\mu_2 S_{2z}} - \left(\frac{iK_z^2\Delta_z}{\mu S_z}\right)_{p=0}. \tag{30}$$

The reflection and transmission coefficients for TM waves can be similarly derived.

For consistency check of the solution above, when the single interface is removed by setting the two media to be the same, and with the fact that $-iK_z\Delta_z = \exp(-i\delta_z) - \exp(i\delta_z)$, the reflection coefficient becomes identically zero, and the transmission coefficient equals one.

With the reflection and transmission coefficient for a single interface derived, one can use a recursive scheme as in (Chew, 1995) to derive the reflection coefficient of a multilayered PML medium. The solution is also consistent with the direct use of finite difference method whereby the problem is first reduced to a one-dimensional one. The resultant matrix equation, which is a tridiagonal, is then tenable to a recursive solution.

4. A Perfectly Matched Interface?

A perfectly matched interface exists in the continuum space, as has been proved by previous works in this area. It will be prudent to investigate if this exists in the discretized space in accordance with the above analysis.

The phase matching condition implies that $K_{1x} = K_{2x}$, and $K_{1y} = K_{2y}$. With the choice that $\mu_1 = \mu_2$, $\epsilon_1 = \epsilon_2$, $S_{1x} = S_{2x}$, and $S_{1y} = S_{2y}$, and from the dispersion relation, one arrives at

$$\frac{K_{iz}}{S_{iz}} = \left(K_i^2 - \frac{K_{ix}^2}{S_{ix}^2} - \frac{K_{iy}^2}{S_{iy}^2}\right)^{1/2}, i = 1, 2. \tag{31}$$

The above implies that

$$K_{1z}/S_{1z} = K_{2z}/S_{2z}. \tag{32}$$

Then, the reflection coefficient becomes

$$R^{TE} = \frac{e^{-i\delta_{1z}} - e^{i\delta_{2z}} - e^{-i\delta_{0z}} + e^{i\delta_{0z}}}{e^{i\delta_{1z}} + e^{i\delta_{2z}} + e^{-i\delta_{0z}} - e^{i\delta_{0z}}}. \tag{33}$$

Hence R^{TE} is in general not zero when the conditions for perfectly matched interface from the continuum case is chosen. Due to the complexity of the expression for the reflection coefficient, it is unlikely that a condition can be found such that $R^{TE} = 0$ for all frequencies and all angles.

When $\Delta_z \to 0$, all the δ_z's become very small, and the above becomes

$$R^{TE} \sim i\delta_{0z} - i(\delta_{1z} + \delta_{2z})/2. \tag{34}$$

In the above δ_{0z} is its value at $p = 0$. Since $\delta_z = k_z\Delta_z/2$, the reflection coefficient is proportional to Δ_z in this limit. Also,

$$\delta_z \sim \frac{S_z\Delta_z}{2}\sqrt{K^2 - \frac{1}{S_x^2}K_x^2 - \frac{1}{S_y^2}K_y^2} + O(\Delta_z^3).$$

If we pick the S_z at the interface to be the average of the material properties of the two media, viz., $S_{0z} = 0.5(S_{1z} + S_{2z})$, then $\delta_{0z} \approx 0.5(\delta_{1z} + \delta_{2z})$, and the leading order term in (34) vanishes. In this case, assuming that $S_x = S_y = 1$, then

$$R^{TE} \sim \frac{\Delta_z^2}{16}\left(S_{2z}^2 - S_{1z}^2\right)\left(K^2 - K_x^2 - K_y^2\right) + O(\Delta_z^3). \tag{35}$$

Notice that the residual error is of second order, and is proportional to the contrast of the two media. The second-order error is consistent with the fact that the finite difference method incurs second order error if done correctly.

5. Numerical Simulations—Discrete-Space Theory

In the following simulation, unless otherwise stipulated, a_z is assumed to be 1 throughout for simplicity. a_z can be chosen to differ from 1 to give the PML medium an added degree of freedom if desired, in order to absorb the evanescent wave well.

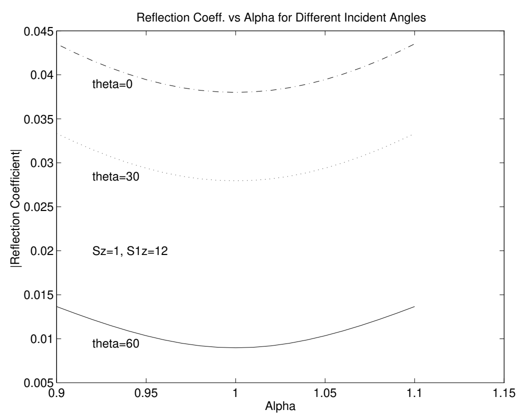

Figure 1. *Residual reflection coefficient for a half space with different stretching variables in the z direction, S_z and S_{1z}, and with different incident angle as a function of α. The frequency is 30 GHz and the discretization size $\Delta = 0.01$ cm. The reflection coefficient does not vanish due to discretization error.*

In Figure 1, the reflection coefficient for a single interface is studied. Here, it is assumed that $S_{0z} = 0.5\alpha(S_{1z} + S_{2z})$. According to the analysis, $\alpha = 1$. At an interface where both S_z and S_{1z} are real, it is seen that this choice of α is optimal for different angles of incidence. However, the reflection coefficient could not be made to vanish with different choice of α. The residual reflection coefficient comes mainly from the discretization error of the continuum equation. As the angle of incidence increases, the residual error decreases, reducing the reflection coefficient. The reason being that as k_z decreases, λ_z increases increasing the effective discretization density per wavelength in the z direction.

In Figure 2, S_{1z} is assumed complex with a large loss tangent of 12. In this case, a proper choice of α could make the reflection coefficient almost zero. The reason is that the wrong choice of α here leaves a residual first-order error that cancels the higher-order errors. It fails to happen in the previous case, because then, the two errors are out of phase whereas with a large loss tangent, this error could be in phase and made to cancel each other. However, the optimal α varies

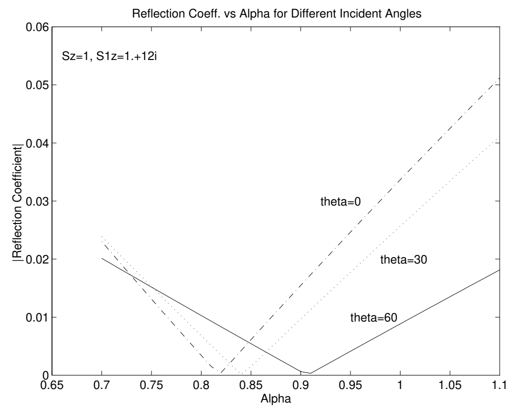

Figure 2. *The same case as Figure 1, except that the stretching parameter in medium 2 is complex with a large loss tangent, $S_{1z} = 1 + 12i$. In this case, the wrong choice of α introduces deliberate first-order error to cancel the second-order error so that the reflection coefficient becomes very small for certain α.*

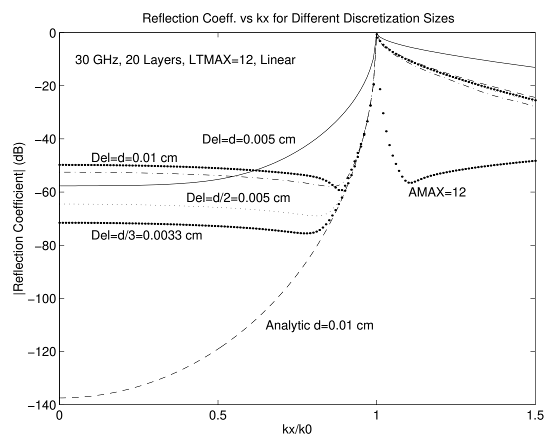

Figure 3. *A PML medium with a linear profile. The reduction of discretization size (Del=Δ) without reducing the PML thickness reduces the reflection coefficient. The solid line case corresponds to a simultaneous reduction of Δ and PML thickness. An extra case for $\Delta = d = 0.01$ cm where a_z is given the same linear profile as the loss tangent shows the absorption of the evanescent waves.*

as a function of angle. Therefore, no one universal α exists for all angles and all frequencies. In the following simulations, $\alpha = 1$.

Figure 3 shows the effect of discretization on the reflection coefficient when the PML is used as an absorber. In this example, the frequency is assumed to be 30 GHz, and 20 PML with a linear profile is used. The maximum loss tangent (LTMAX$=|\Omega_x/(\hat{\Omega}_t a_x)|$) of the PML is 12. The continuum space theory (analytic) indicates that close to -140 dB absorption is possible with such layers. Two numerical experiments are performed here: One whereby the layer thickness d is kept constant at 0.01 cm, and the discretization size Δ is reduced. In this case, the smaller values of Δ bridge the gap between the continuum-space theory and the discrete-space theory. In the solid-line case, the layer thickness is reduced the same time when the discretization size is reduced. For some k_x's, close to normal incidence, it outperforms the constant d case, and is inferior when close to grazing incidence. For the $\Delta = d = 0.01$ cm case, when a_z is given a the same linear profile as the loss tangent with $a_{z,max} = AMAX = 12$, it is seen that the evanescent spectrum is absorbed well also. This can be understood easily from Equation (19).

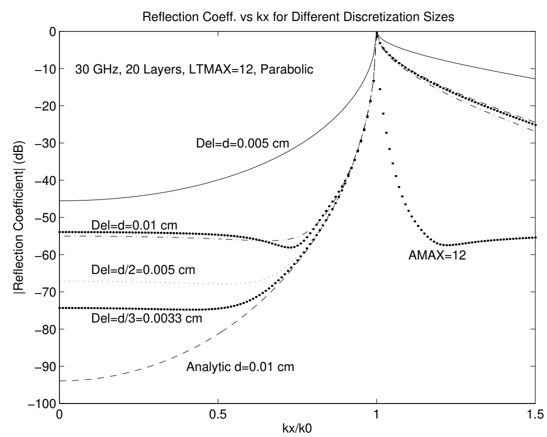

Figure 4. *The same case as Figure 3, except that a parabolic profile is used. The simultaneous reduction of PML thickness and Δ does not improve the result. An extra case for $\Delta = d = 0.01$ cm shows the absorption of evanescent waves when a_z is given the same parabolic profile as the loss tangent.*

Figure 4 shows the same experiment for a parabolic profile. In this case, the continuum space theory (analytic) predicts lower absorption compared to the linear profile. The reason is that the absorption of the PML in the continuum theory is proportional to the area under the profile via the equation

$$e^{i\int_0^L K_z(z)dz},$$

where L is the total thickness of the PML and $K_z(z)$ is a complex number. Therefore, less area exists under a parabolic profile compared to a linear profile. However, the gap between the discrete-space theory and the continuum-space theory is smaller compared to the previous case. For the same discretization, the parabolic profile outperforms the linear profile slightly in this example. The explanation is that in a parabolic profile, the loss is changed more gradually from a lossless medium to a lossy medium, so that the contrast between adjacent layers is smaller. This tends to mitigate the discretization error. However, in the example whereby the PML thickness d is decreased simultaneously with the discretization size Δ, the PML does not perform as well compared to the previous figure. The reason being that the effective area under the profile decreases more rapidly in this case as the PML thickness is decreased. Notice that when a_z is given the same parabolic profile as the loss tangent with the maximum value of 12, the evanescent spectrum is well absorbed.

In the continuum theory, it is well-known that the absorption will increase indefinitely with the increase in the loss tangent of the PML since no reflection occurs at any of the interfaces. However, this is not true in the discrete-space theory. In

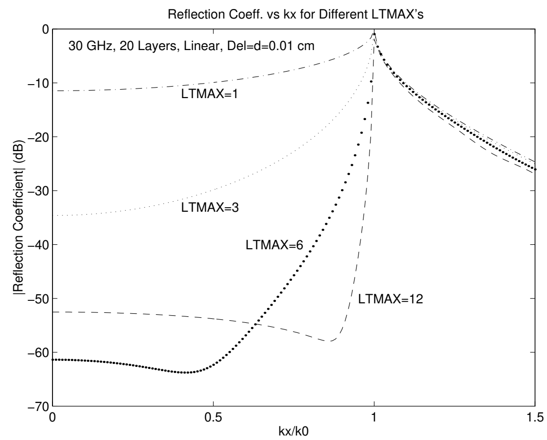

Figure 5. *The reflection coefficient for different amount of loss in the PML medium. The increase of the loss in the PML by increasing the maximum loss tangent (LTMAX) of a linear profile does not improve the reflection coefficient indefinitely.*

Figure 5, it is shown that increasing the loss tangent of the profile by increasing the maximum loss tangent (LTMAX) aids in the absorption initially, but eventually will saturate because increasing the loss profile will eventually increase the contrast between adjacent layers, accentuating the discretization error as indicated by Equation (35).

6. Optimization of PML for FEM Applications

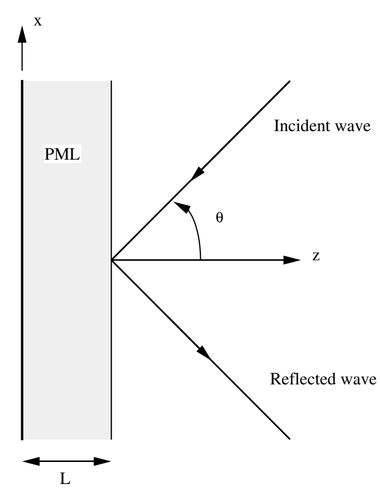

Figure 6. *Plane wave reflection by a metal backed PML.*

Much of the salient features of PML media observed in the finite difference method are also observed in the finite element method. Since the PML contains several parameters, it is necessary to find a set of optimal parameters to achieve the best performance. For this purpose, we consider the problem where a plane wave is incident on a PEC-backed PML obliquely at an angle θ with the z-axis (Figure 6). For TM case, this incident wave can be represented by

$$E_y^{inc}(x,z) = E_0 e^{-ik_0 z\cos\theta + ik_0 x\sin\theta}. \tag{36}$$

This plane wave will be reflected by the PML and the reflected field can be represented by

$$E_y^{ref}(x,z) = R^{TM} E_0 e^{ik_0 z\cos\theta + ik_0 x\sin\theta}, \tag{37}$$

Therefore, for $z \geq L$ the total field is

$$E_y^{total} = E_y^{ref} + E_y^{inc}, \tag{38}$$

from which we obtain

$$\left[\frac{dE_y}{dz} - ik_0\cos\theta E_y\right]_{\text{at } z=L+0} = -2ik_0\cos\theta E_0 e^{-ik_0 L\cos\theta}, \tag{39}$$

or through the field continuity condition

$$\left[\frac{1}{S}\frac{dE_y}{dz} - ik_0\cos\theta E_y\right]_{\text{at } z=L-0} = -2ik_0\cos\theta E_0 e^{-ik_0 L\cos\theta}. \tag{40}$$

The field in the PML region can be shown to satisfy the differential equation

$$\frac{d}{dz}\left(\frac{1}{S_z}\frac{dE_y}{dz}\right) + k_0^2 S_z(1-\sin^2\theta)E_y = 0, \qquad 0 \leq z \leq L. \tag{41}$$

This differential equation, together with the boundary condition at $z = L$ given in (40) and $E_y = 0$ at $z = 0$, can be solved using the 1D FEM, from which we obtain the field in the region $0 \leq z \leq L$.

The reflection coefficient can then be calculated as

$$R^{TM} = \frac{E_y(z=L) - E_0 e^{-ik_0 L\cos\theta}}{E_0 e^{ik_0 L\cos\theta}}. \tag{42}$$

Similar procedure can be employed to calculate R^{TE}.

It is obvious that the reflection coefficients, R^{TM} and R^{TE}, are functions of k_0, θ, S_z, and L (S_z is a function of z). For example, R^{TM} can be written as

$$R^{TM} = f_1(k_0, \theta, S_z, L). \tag{43}$$

If the number of PML is fixed to be N and the form of S_z is given such as

$$S_z = 1 + i\left(\frac{z-L}{L}\right)^m L_{t\,\max}, \tag{44}$$

where m can be 0, 1, 2, or 3, then R^{TM} can be written as

$$R^{TM} = f_1(k_0, \theta, L_{t\,\max}, \Delta), \tag{45}$$

where Δ is the thickness of each PML,

$$\Delta = \frac{L}{N}. \tag{46}$$

In the above $L_{t\max}$ is the maximum loss tangent. Similarly, we have

$$R^{TE} = f_2(k_0, \theta, L_{t\max}, \Delta). \tag{47}$$

For a given frequency, we can define an object function

$$R = \int_0^{\theta_{\max}} [|f_1| + |f_2|] \, d\theta = R(L_{t\max}, \Delta), \tag{48}$$

where $\theta_{\max}$ defines the range of the incident angle to be considered.

To find the best PML, we can employ one of optimization schemes to minimize R with respect to $L_{t\max}$ and Δ. In this work, we use Powell's method for this purpose (Press et al., 1992; Jin et al., 1992).

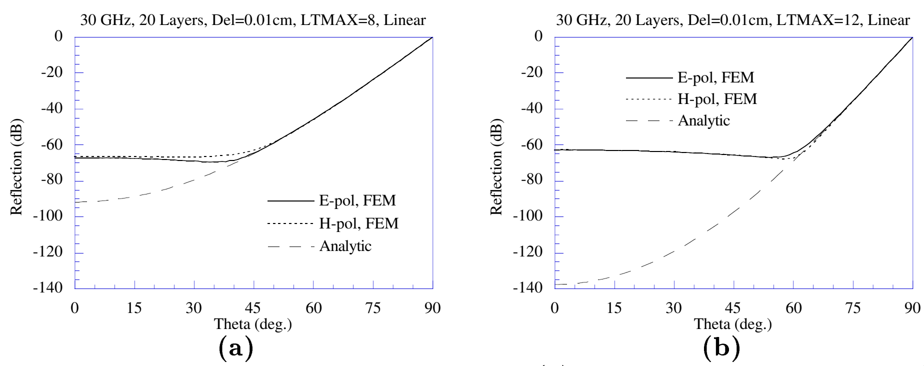

Figure 7. *Reflection coefficient of a PML. (a) Δ = 0.01 cm, LTMAX = 8. (b) Δ = 0.01 cm, LTMAX = 12.*

First, to corroborate the results shown in Figures 3 and 4, the reflection coefficients are computed for a linear 20-layer PML with $\Delta = 0.01$ cm at 30 GHz. The results are given in Figure 7 for two different LTMAX, compared with the theoretical prediction based on the continuum theory. Similar phenomena are observed here for the finite element solution as in the finite difference solution.

Next, we show some results obtained using the optimization scheme. In all these results, the number of layers is fixed at 20, the frequency is assumed to be at 30 GHz, and the loss tangent is chosen to be a parabolic function. The parameters to be optimized are Δ and LTMAX for a chosen $\theta_{\max}$. Figure 8 shows the results obtained for $\theta_{\max} = 40$, 60, and 80 degrees. As can be seen, one is able to find a set of optimal parameters, Δ and LTMAX, to achieve the best performance within $\theta_{\max}$. As is expected, the overall reflection is smaller for a smaller $\theta_{\max}$ and for a large $\theta_{\max}$ the performance is slightly compromised. It is also interesting to note that contrary to the common belief that Δ should be set at 0.1λ, it is found that the best performance is achieved with $\Delta \approx 0.01\lambda$—$0.02\lambda$.

In our optimization scheme described above, we have not specified the frequency range to be optimized since we expect that the PML will have a wide frequency band, as predicted theoretically. This is indeed true, as can be seen in Figure

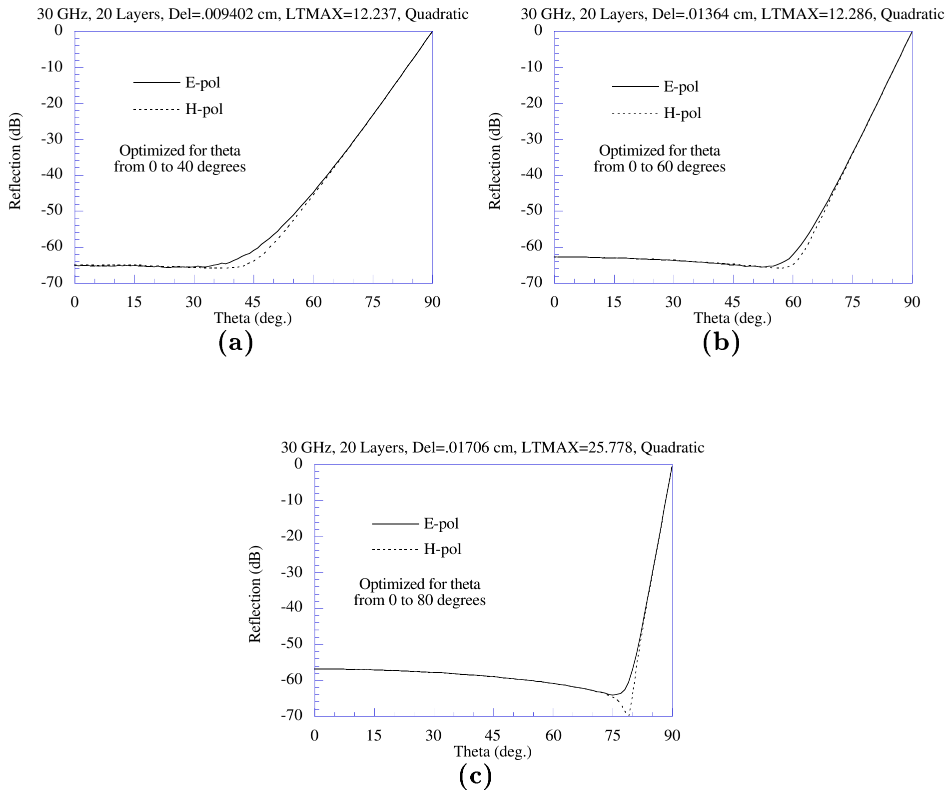

Figure 8. *Reflection coefficient of an optimized PML. (a) Optimized for θ from 0 to 40 degrees. (b) Optimized for θ from 0 to 60 degrees. (c) Optimized for θ from 0 to 80 degrees.*

9, where the reflection coefficient is shown for two angles of incidence for a PML optimized at 30 GHz. The reflection coefficient is nearly a constant across the entire frequency range, even at very low frequencies.

7. Application of PML to FEM Solution of Waveguide Discontinuity Problems

To illustrate the application of the PML, we consider the waveguide discontinuity problem shown in Figure 10(a), where a discontinuity (either geometrical, or material, or both) exists at the joint of two parallel plate waveguides. To solve this problem using the FEM, we truncate the solution region using the PML, at the two ends of the waveguide, as shown in Figure 10(b).

For H-polarization, the field in the entire region is given by

$$\frac{\partial}{\partial z}\left(\frac{1}{S_z\epsilon_r}\frac{\partial H_y}{\partial z}\right)+\frac{\partial}{\partial x}\left(\frac{S_z}{\epsilon_r}\frac{\partial H_y}{\partial x}\right)+k_0^2S_z\mu_rH_y=0, \tag{49}$$

where $S_z = 1$ for non-PML region. To excite an incident wave, we place a magnetic current sheet $\mathbf{M}$ at the front of the PML on the left-hand side. This problem can be

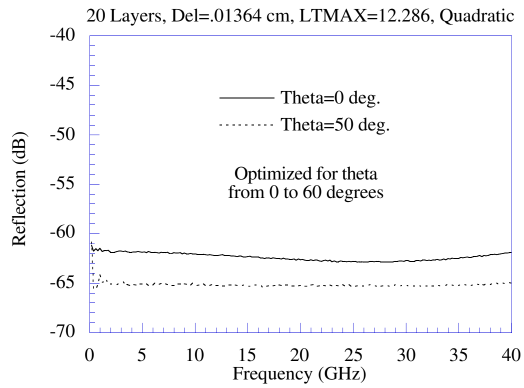

Figure 9. *Reflection coefficient of a PML optimized at 30 GHz.*

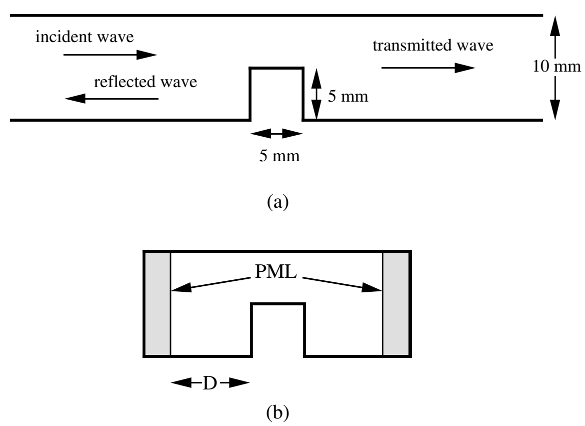

Figure 10. *(a) A waveguide discontinuity problem. (b) PML truncation.*

analyzed easily using a 2D FEM. Once we have obtained the solution, the reflection and transmission coefficients for the dominant mode can be obtained as

$$R = \frac{1}{H_0 e^{-ik_0 z_1}} \int_0^a \left[H_y(z_1) - H_y^{inc}(z_1) \right] \, dx, \tag{50}$$

$$T = \frac{1}{H_0 e^{ik_0 z_2}} \int_0^b H_y(z_2) \, dx, \tag{51}$$

where z_1 denotes a point between the discontinuity and the PML on the left-hand side, z_2 denotes any point between the discontinuity and the PML on the right-hand side, a and b represent the width of the waveguide at z_1 and z_2, respectively.

Representative results are given in Figure 11 where both the reflection and transmission coefficients associated with the dominant mode are shown for a dominant mode incidence. These results were obtained with the optimized PML given in Figure 10 and the absorbing surface of the PML was placed 10 mm and 12.5 mm

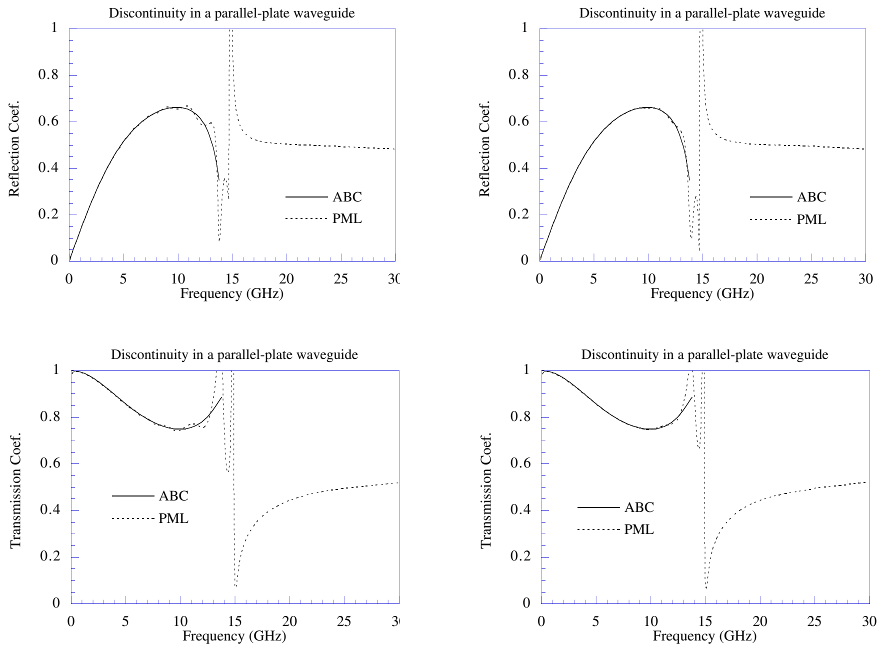

(a) **(b)**

Figure 11. *Reflection and transmission coefficients for the dominant mode with the PML placed (a) 10 mm and (b) 12.5 mm away from the discontinuity.*

away from the discontinuity for Figures 11 and 12, respectively. These results were compared with the data obtained using the absorbing boundary condition (ABC) which was derived for the dominant mode (Jin, 1993) and thus is applicable only to the frequencies below the cut-off of the second mode (15 GHz). The ABC was applied 15 mm away from the discontinuity and its result has an accuracy better than 1% from 0 to 12 GHz. The sampling rate for both ABC and PML solutions was 2 points/mm in the non-PML region. It is clear that to obtain accurate result, the PML must be placed sufficiently far away from the discontinuity. The reason being that PML does not work as well for evanescent waves compared to plane waves. It is also obvious that the PML is not applicable at cut-off since it has a reflection coefficient close to one at the grazing incidence.

8. Conclusions

The PML has been analyzed using finite-difference equation. It is shown that a perfectly-matched interface does not exist in the discretized space due to discretization errors of the continuum equations. The errors are of second order, and are proportional to the contrast between two PML media. These errors decrease when the angle of incidence is close to grazing because the discretization density per wavelength is higher there.

A stack of PML media can be used to design material absorbers for FDTD simulations. A PML tapered by parabolic profile is found to work better than one tapered by a linear profile. Since the discretization error is proportional to contrast, increasing the loss tangents of the PML does not reduce the reflection coefficient indefinitely.

The finite-element simulation of PML is shown to exhibit similar phenomena as the finite difference case. The Powell method can be used to design optimal PML for absorption. With 20 layers of PML, close to -60 dB absorption is possible from 0 to 80 degrees. The absorption exhibits extremely broad bandwidth down to static.

A simulation of PML for the absorption of waves is performed for 2D finite element method in a waveguide with a junction discontinuity. It is observed that the further the PML is placed away from the waveguide junction, the better is the simulation result. The reason being that PML does not work as well for evanescent waves. PML is observed to fail close to cut-off because then, the PML does not absorb well.

References

Berenger, J.-P., "A perfectly matched layer for the absorption of electromagnetic waves," *J. Computational Physics*, **114**, 185–200, 1994.

Chew, W. C., "Electromagnetic theory on a lattice," *J. Applied Physics*, **75**, 10, pp. 4843-4850, May 1994.

Chew, W. C., *Waves and Fields in Inhomogeneous Media.* Van Nostrand, New York, 1990 (reprinted by IEEE Press, 1995).

Chew, W. C. and W. H. Weedon, "A 3D perfectly matched medium from modified Maxwell's equations with stretched coordinates," *Micro. Opt. Tech. Lett.*, **7**, 599-604, 1994.

Chew, W. C., W. H. Weedon, and A. Sezginer, "A 3-D perfectly matched medium by coordinate stretching and its absorption of static fields," *ACES Digest*, Monterey, CA, pp. 482-489, March, 1995.

Gribbons, M., S. K. Lee, and A. C. Cangellaris, "Modification of Berenger's perfectly matched layer for the absorption of electromagnetic waves in layered media," *ACES Digest*, Monterey, CA, pp. 498-503, March 1995.

Jin, J. M., *The Finite Element Method in Electromagnetics.* John Wiley & Sons, New York, 1993.

Jin, J. M., J. L. Volakis, and V. V. Liepa, "Fictitious absorber for truncating finite element meshes in scattering," *IEE Proc. H*, **139**, 5, pp. 472-476, 1992.

Katsz, D. S., E. T. Thiele, and A. Taflove, "Validation and extension to three dimensions of the Berenger PML absorbing boundary condition for FD-TD meshes," *IEEE Micro. Guided Wave Lett.*, **4**, 8, pp. 268-270, 1994.

Mittra, R. and Ü. Pekel, "A new look at the perfectly matched layer (PML) concept for the reflectionless absorption of electromagnetic waves," *IEEE Micro. Guided Wave Lett.*, **5**, 3, pp. 84-86, 1995.

Navarro, E. A., C. Wu, P. Y. Chung, and J. Litva, "Application of PML superabsorbing boundary condition to non-orthogonal FDTD method," *Electronics Lett.*, **30**, 20, pp. 1654-1656, 1994.

Press, W. H., S. A. Teukolsky, W. T. Vetterling, and B. P. Flannery, *Numerical Recipes,* 2nd ed. Cambridge: Cambridge Univ. Press, 1992.

Sacks, Z. S., D. M. Kingsland, R. Lee, and J.-F. Lee, "A perfectly matched anisotropic absorber for use as an absorbing boundary condition," *IEEE Trans. Antennas Propag.*, vol. 43, no. 12, pp. 1460-1463, 1995.

Taflove, A., "Review of the formulation and applications of the finite-difference time-domain method for numerical modeling of electromagnetic wave interactions with arbitrary structures," *Wave Motion,* **10**, 6, pp. 547-582, 1988.

Yee, K. S., "Numerical solution of initial boundary value problems involving Maxwell's equation in isotropic media," *IEEE Trans. Antennas Propag.*, **AP-14**, 302–307, 1966.